

THE EXPANSION OF THE AMORPHOUS PART
OF THE CRAB NEBULA

Hugh M. Johnson

This paper presents observations of the expansion of the amorphous mass of the Crab Nebula from 1899 to 1963. First, however, it summarizes some of the earlier observations of the Crab Nebula so as to show the relevance of the new data.

Lampland (1921) added the Crab Nebula to a short list of variable nebulae then known, namely the comet-shaped nebulae NGC 1555, NGC 2261, and NGC 6729. Using a blink comparator on a series of 40-inch Lowell reflector plates exposed in 1913-21, he discovered changes in form and possibly changes of the position of the structure of the nebula, and described some of them. Lampland considered that the Crab Nebula belongs to an entirely different class from the comet-shaped nebulae, a point which has subsequently become arguable (Gurzadyan 1960).

Duncan (1921, 1939) measured the positions of 20 nebulous points in the Crab Nebula on Mount Wilson 60-inch reflector plates exposed in 1909-1938, and he discovered a systematic expansion from a center within the nebula, illustrated in Figure 1. Almost by astrometric necessity for a 29-year baseline, these 20 points were parts of the sharp filamentary system of the nebula rather than of the amorphous mass, although the filamentary structure does not stand out very distinctly in ordinary blue-sensitive plates.

Slipher's (1916) observations of doubled bright lines in the spectrum of the Crab Nebula were confirmed by Sanford (1919), who also detected the continuous spectrum. Mayall (1937) measured several radial velocities in the nebula and compared them with Duncan's 1921 astrometry. It was apparent that the bright-line spectrum originates in the filaments and the continuous spectrum in the amorphous mass. It was also apparent that the amorphous mass is not a reflection nebula because no sufficiently bright central star was visible and there was no extinction of the red (far-side) components of the doubled bright lines. The nature of the spectral continuum remained unknown until Shklovsky (1953) proposed that it was synchrotron radiation, and the predicted polarization of the light was confirmed. Woltjer (1958) showed that synchrotron radiation below the Lyman limit probably accounts for the excitation of the filamentary gas. He also showed that the total mass of interstellar gas swept by the shell of filaments is negligible in comparison with the mass of the filaments, and that the dynamical effects of the interstellar atoms on the shell are rather small.

There is no evidence that the filaments contribute synchrotron radiation in the system. In passbands selected to be fairly free of monochromatic emissions they

The National Radio Astronomy Observatory is operated by the Associated Universities, Inc., under contract with the National Science Foundation.

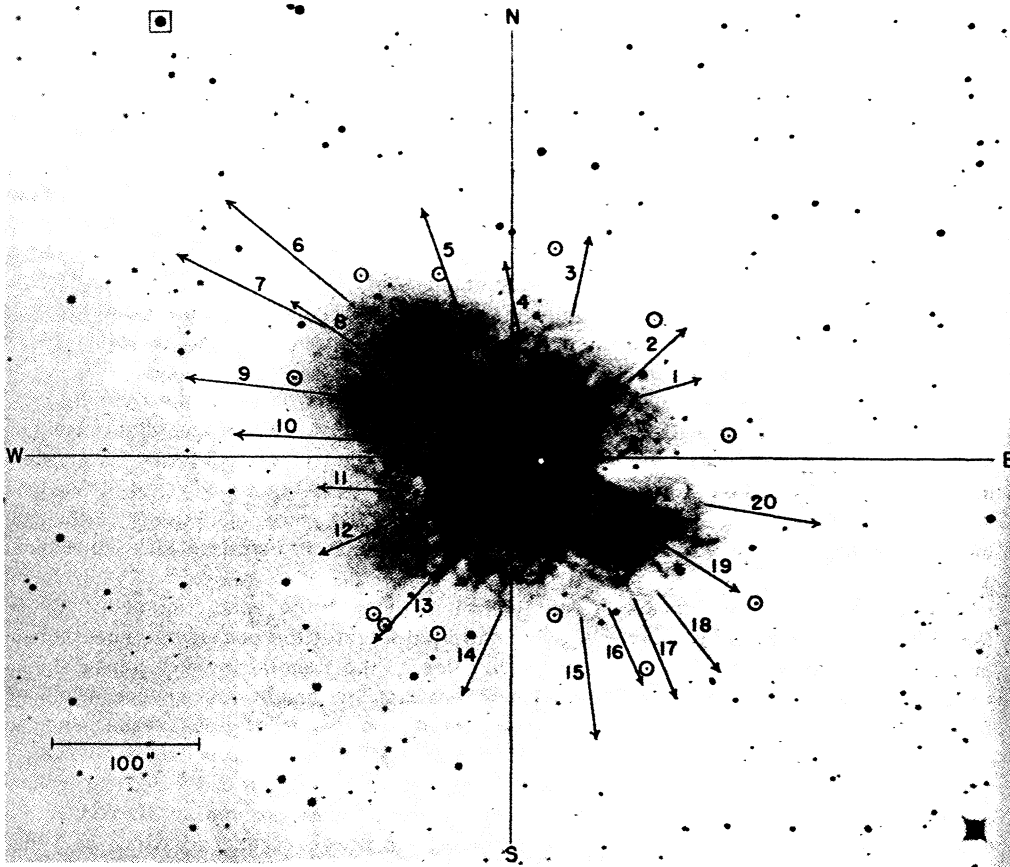


Fig. 1 -- The expansion of the filamentary structure of the Crab Nebula (Duncan 1939). The vectors indicate the motion of 20 filamentary points in 500 years. The white dot is the center of expansion. Comparison stars are circled. The star in a square shows conspicuous proper motion. Reproduced by courtesy of the author and publisher, The University of Chicago Press. Copyright 1939 by The University of Chicago.

lose practically all contrast with the amorphous mass (Baade 1942, 1956). That is, no continuum -- synchrotron-type or otherwise -- has been detected in the filaments. They do not contribute to the polarization of the light of the Crab Nebula according to a direct test of [O III] λ 5007 (Hiltner 1957). The only directly observed connections between the filamentary and amorphous systems that comprise the nebula are the following:

1. There is a general (but not detailed) spatial association. According to Baade (1942) the filaments fill an almost perfect ellipse with $a = 178''$, $b = 120''$, which he calls the outer envelope around the inner S-shaped amorphous mass. However, the outer isophotes of Woltjer's (1957) map of Baade's 200-inch plates are more nearly circular and extend as much as 220" in radius. These isophotes refer to the continuum and show that the filamentary shell is embedded in a more extensive amorphous mass. Little's (1963) summary of the radio data between λ 8 mm and 7.9 m shows that the half-brightness width has been measured to be 2:5 to 8:5 east-west and 3:4 to 8:5 north-south; the variation with frequency is not well defined.

2. There may be some relation between the projection of the electric vectors of the polarized continuum and the filaments, but it is not clear how it should be described. Woltjer (1958) says that at a number of places in the outer parts of the nebula the projected electric vectors appear to emerge radially from a certain point, and this point is then situated in a filament (as though the filaments carry a current and are surrounded by circular lines of force). Shajn, Pikelner, and Ikhsanov (1955), and Mme. Martel (1958), find that the direction of the projected electric vectors are characteristically normal to the filaments (as though the magnetic field is parallel to the filaments). Münch (1958) has noticed that many of the filaments are oriented in a direction nearly parallel to that of the electric vector (as though the magnetic lines of force are normal to the filaments).

The writer's opinion is that the electric vectors appear to be normal to streaks of the amorphous continuum, but that the directions of the electric vectors and filaments are practically independent.

3. Oort and Walraven (1956) measured the transverse motion of a wisp of the amorphous mass and found it to be practically the same as that of the ordinary unpolarized filaments. This confirmed earlier measures of the motion of seven probably amorphous details near the major axis of the nebula by Deutsch and Lavdovsky (1940).

The data of the preceding paragraph are important because many discussions of the Crab Nebula (and other radio sources) combine the kinematics of the filamentary system and the characteristics of the amorphous source of synchrotron radiation. Not too much weight can be attached to the single proper-motion datum of Oort and Walraven, in the light of the following interesting feature of the Crab Nebula which they announce in the same paper. It is the occurrence of the moving light ripples observed by Baade and related to the earlier observations of Lampland (who did not actually specify the expansion of the nebula). The transverse speed of Baade's ripples was roughly one-tenth the speed of light, and the time scale of their existence was three months. Changing details of a slower and larger scale than Baade's ripples are known but not published (Mayall 1962). The work of Deutsch and Lavdovsky is extremely interesting but it is rather sketchy and lacking in controls of the measure of the apparent motion of the details.

The rest of this paper gives the results of the writer's attempt to measure the expansion of the amorphous mass of the Crab Nebula over a period of about 60 years. The long baseline and the coarse nature of prominent amorphous features at once remove the necessity to use a very large telescope. Table 1 lists the plates that will be considered. They were all exposed in the 36-inch Crossley reflector of the Lick Observatory, those of 1963 with the very kind permission of Dr. G. H. Herbig, who also allowed the use of the plates of Table 1 in the Hilger microphotometer of the Kitt Peak National Observatory and later the study of them at the National Radio Astronomy Observatory. The writer wishes to thank Dr. Herbig and others in the Lick Observatory for much assistance and many courtesies. The writer also extends thanks to Dr. N. U. Mayall for permission to use the offices of the KPNO in this work.

It is obvious that, in order to compare the old plates with new ones, the latter ought to be given a range of characteristics that include the old characteristics, so that the differences in the size of the nebula would not merely reflect differences in the plate characteristics. The following characteristics were controlled: (1) Spectral sensitivity. (2) Exposure or image density. (3) Contrast. On the other hand certain variations, such as those in plate graininess, seeing, or guiding errors, were not considered to be important if the scanning aperture of the analyzing microphotometer were made rather large in comparison with the smaller star images of the worst plates.

The importance of matching spectral sensitivity lies chiefly in maintaining the relative contributions of the continuum and the monochromatic emissions to the structure of the image. To begin with, one would like to have a passband that suppresses monochromatic emissions altogether, but the old plates of 1899-1914 do not meet the desideratum, and the new plates must follow suit. Fortunately, according to Baade (1942), a conservative estimate indicates that in the photographic region the amorphous mass (continuum) contributes more than 80 per cent of the total light. He specifies the photographic region as $\lambda\lambda$ 3600-5000 Å. It is well known that aluminum reflects nearly uniformly in this region and down to the atmospheric limit, whereas the reflectance of one silver coat drops to half its value at λ 4000 Å by λ 3300 Å, while the transmittance of 2 mm of GG 13 (Schott glass) filter drops to half its value at λ 4000 Å by about λ 3870 Å, according to an interpolation of the manufacturer's data. Silvered mirrors, whether one or two, therefore appear to define a passband that is intermediate between aluminum and aluminum with 2 mm of GG 13 filter. In particular [O II] λ 3727, the strongest monochromatic emission in the Crab Nebula, is reflected by aluminum but is fairly well filtered out by the GG 13. Even so, Figure 2 shows that the tracing of a Crossley plate with GG 13 filtering looks much like the tracing of an unfiltered plate. Measures of the tracings confirm that the distribution of light in the Crab Nebula is not sensitive to the short-wavelength cut-off of the passband. This experience indicates also that small changes in atmospheric transparency should not cause apparent changes in the image. The sky of 1963 was quite clear.

It is unfortunate that no plates approximately like those of IIa-O emulsion with or without the GG 13 filter were exposed in the Crossley telescope between 1914 and 1963. Mayall exposed some plates with special passbands in this period, one of which, labelled NM 510, is listed in Table 1 and measured in the same way as the other plates in this paper. The passband of plate NM 510 ran from about λ 5400 Å redward to include $H\alpha$. Filamentary structure is much more prominent on it than on the other plates, yet the amorphous features of the blue-sensitive plates are recognizable on

TABLE 1
SOME CROSSLEY REFLECTOR PLATES OF THE CRAB NEBULA*

Date	Emulsion	Filter	Exposure	Development**	Plate No.	Observer
1899 Dec. 24†	Not known	None	120 ^m	Not known	-----	Keeler
1899 Dec. 26	Not known	None	180	Not known	-----	Keeler
1914 Oct. 24	Seed 27	None	150	Not known	-----	Curtis
1938 Jan. 5	H α spec. hyp.	Wratten 16	60	Not known	NM 510	Mayall
1963 Jan. 20	II a-O	None	45	3 ^m	CD 782	Johnson
1963 Jan. 20	II a-O	2 mm GG 13	45	3	781	"
1963 Jan. 21	II a-O	2 mm GG 13	10	5	785	"
1963 Jan. 21	II a-O	2 mm GG 13	10	3	786	"
1963 Jan. 21	II a-O	2 mm GG 13	20	3	787	"
1963 Jan. 22	II a-O	2 mm GG 13	20	3	791	"
1963 Jan. 22	II a-O	2 mm GG 13	20	8	792	"
1963 Jan. 22	II a-O	2 mm GG 13	10	8	793	"
1963 Jan. 22	II a-O	2 mm GG 13	40	8	795	"
1963 Jan. 22	II a-O	2 mm GG 13	40	5	794	"

* Newtonian focus before 1905, then prime focus. Silvered before 1933, then aluminized.

**The writer's plates were developed in D-19 at 63-64° F, with continuous agitation.

† Reproduced in Plate 9 of the Lick Observatory Publications, 8, 1908.

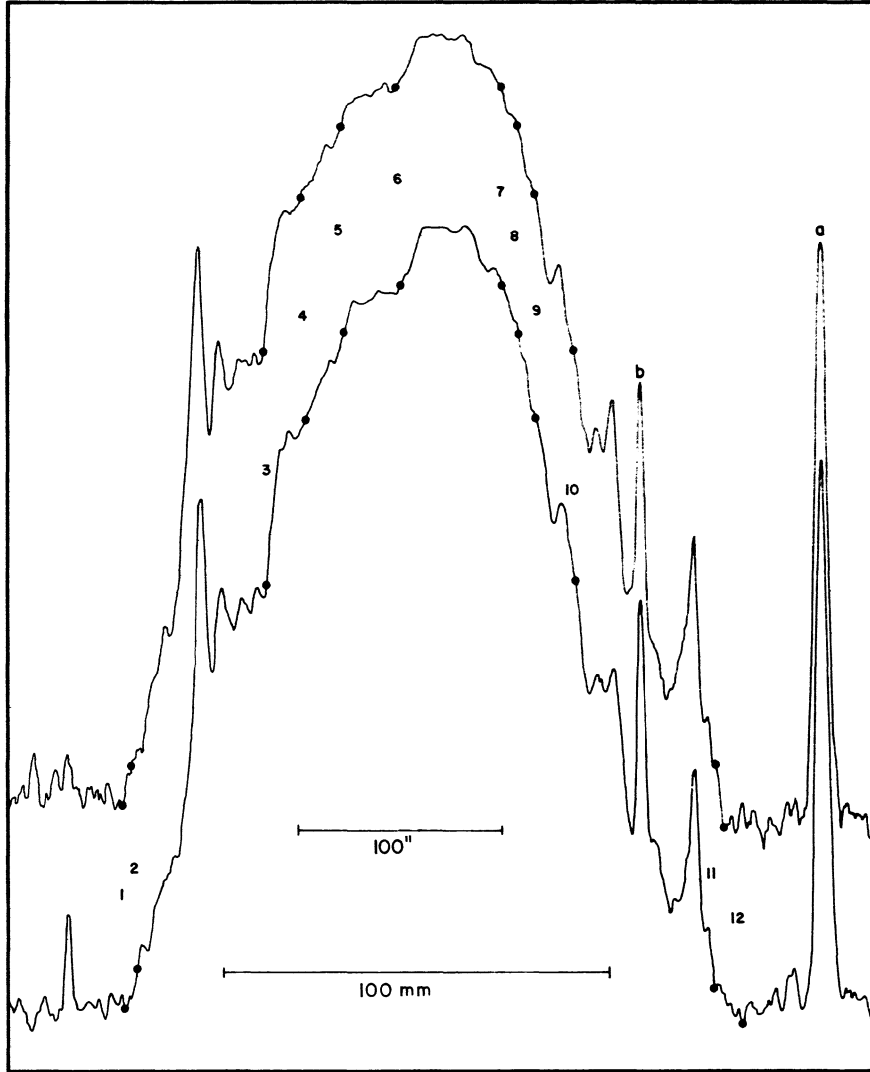


Fig. 2 -- A drawing made from microdensitometer tracings of plates CD 782 (top, no filter) and CD 781 (GG 13 filter) on track 2 to show the small dependence of the features on the short-wavelength cut-off. The calibration stars a and b are labelled, and the twelve nebular features, whose measures appear in Table 2, are marked as dots on the graphs and labelled with the numbers between the two graphs. The outer parts of the sky background are left out. Calibration star c is also excluded. The graph is photographic density, integrated in a scanning aperture about 3.7 mm in size on the original scale of the chart, versus track position. Infinite density lies 21 mm above the peak of CD 782 and 24 mm above the peak of CD 781.

the tracings of it, and there is little or no systematic deviation of the measures of Mayall's plate from an interpolation between the standard measures.

The long-wavelength cut-off of all of the blue-sensitive plates was assumed to be similar. The conclusion of these paragraphs is that the variation in spectral sensitivity between 1899 and 1963 has little effect on the measures.

The new 20-minute exposures of Table 1 contain images of the Crab Nebula that very nearly match the old images in density. The 40-minute and 10-minute exposures respectively give denser and less dense images. It will be shown that the measured dimensions of the nebula are not dependent on the length of the exposure, except in the outermost parts of lowest brightness. Therefore it should be valid to compare the old and new plates directly, especially if the means of all of the plates are used.

Photographic contrast may be defined in terms of γ , the slope of the characteristic curve, which is the photographic density as a function of the logarithm of the exposure. The new-plate γ -values are known from calibration plates taken from the same box of plates and exposed in a Lick Observatory tube sensitometer placed in the Crossley dome at the same time that the nebula exposures were exposed. These plates were developed in the same developer at the same time as the nebula plates. The only difference between the measured γ -values and the γ -values that actually pertain to the images of the Crab Nebula plus the sky should arise from the difference between the energy distribution of the lamp of the sensitometer and the energy distribution of the Crab Nebula (because γ is ordinarily a function of wavelength). The mean new-plate γ -values, evaluated at density = 0.6 above inherent plate fog are the following: $\gamma(8^m) = 1.43$; $\gamma(5^m) = 1.37$; $\gamma(3^m) = 1.13$. They are given as functions of the time of development. It is impossible to know the γ -values of the old plates for comparison with these values, but in a blink comparator the images of the nebula on the old plates appear to be within the range of the new-plate contrasts. It will be shown that the measured dimensions of the nebula, except perhaps the extremes, are not dependent on γ in the range of values for the new plates, and so it appears fairly safe to compare the old and new plates directly.

The outer dimensions of the amorphous mass can scarcely be found by micrometrical measures of the kind Duncan made of the filaments, and microdensitometer tracings should be less subjective than eye estimates of the centroids of internal details. Such tracings were made on various sections of the image, about three times longer than the image so as to give an ample sky background. Each track was defined by two star images, which also calibrated the scale. Accidental encounters with additional star images on the tracks, except the fourth track, gave further checks on the scale. This scheme of measures does not have the freedom of two-coordinate measures. Instead, only a component of motion (or shift of features) is measured on the tracks. Since these tracks are chosen to fall near Duncan's center of expansion of the filaments (Figure 1), the components will approximate the motions from the same center but not from remote centers. In general, the method follows that of Deutsch and Lavdovsky (1940), but the present data are more extensive and should be more precise.

The scanning aperture of the KPNO microdensitometer is an isocetes trapezoid scanning normal to the parallel sides, which were separated 180μ . The lengths of the parallel sides averaged about the same. The dimensions were in fact made as small as possible without making the signal/noise ratio too small, a somewhat arbitrary matter that was decided after experimentation. The scale of the Crossley re-

flector is $38.6/\text{mm}$, and the major and minor semi-axes of the nebula are about $2' \times 3'$, so that the scanning aperture is about 3.9 to 5.8 per cent as big as the radius. The positions of stars and details in the nebula can be estimated to about one-tenth of these percentages, while the expansion of the filaments has been 8 or 9 per cent of the 1899 radii. The ratio of recorder-chart speed to plate speed was about 20.5, and measurements on the chart were actually made to the nearest millimeter from one of the calibration stars, or from 1.1 to 1.6 per cent of the radius of the nebula.

Figure 3 reproduces one of the Crossley plates to illustrate the scanning tracks, the calibration stars, and the details in the nebula that were selected for measurement on the tracings. A much larger number of tracks could have been laid out, but these are representative. Given six tracks, the problem is to choose points on them that are free of appreciable interference from stars or filamentary light, recognizable at all epochs, and measurable within 1 mm of accuracy on the charts. These criteria do not limit the sample to the actually measured points, but, again, the sample is representative and sufficient to show what the plates contain with little ambiguity. Three types of features in the nebular tracings are measured:

1. In each case the toe of the rise of nebular light above the sky, an ill-defined position because the nebula does not appear to be sharply bounded.
2. Fairly sharp gradients in the brightness of the nebula, usually at large or intermediate radii.
3. Maxima or minima in the brightness, usually at small radii. The examples in Figure 2 show these types of features.

Table 2 lists the measures of distance \underline{s} made on the charts recorded at the microdensitometer. It is divided into the six tracks through the nebula. Column one in each track identifies the plate; columns two and three, respectively, give the distance in millimeters measured from the first to the second \underline{b} or third \underline{c} calibration stars; and the successive columns give the distances measured from the first calibration star to points in the nebula in the same order as the points marked on Figure 3. The measures between the stars in each track would be uniform were the ratio chart speed to plate speed constant from plate to plate.

Tables 3 and 4 arrange some of the data of Table 2 so as to show the effect of varying the exposure and varying the development (contrast) on the measures. In support of statements previously made, these effects are negligible except perhaps on the outermost (toe) measures of the nebula.

The plate of 1914 does not convincingly show departures from uniform motion between 1899 and 1963. Therefore the plate of 1914 and the two plates of 1899 were averaged for an epoch of 1904.9. All of the plates of 1963.1 were also averaged, and the mean values of the measure \underline{s} at this epoch are given in Table 5, together with $\Delta\underline{s}$, representing the mean change of \underline{s} between 1904.9 and 1963.1. Unit $\Delta\underline{s} = 1 \text{ mm}/58.2 \text{ years} = 158 \text{ km/sec}$ at the distance (Woltjer 1958) of 1030 psc. Under columns \underline{b} and \underline{c} , non-zero values of $\Delta\underline{s}$ reveal sample errors in the scale according to the reference stars. (None of the stars has a measurable proper motion.) Unfortunately, one cannot measure the scale errors at the points where the nebular values of \underline{s} are taken, and the number of sample errors is too limited to tell whether the errors are smooth functions of \underline{s} .

We have now to schematize $\Delta\underline{s}$ because the quality of the data probably does not justify a discussion of the motion of individual features. If the apparent motions are

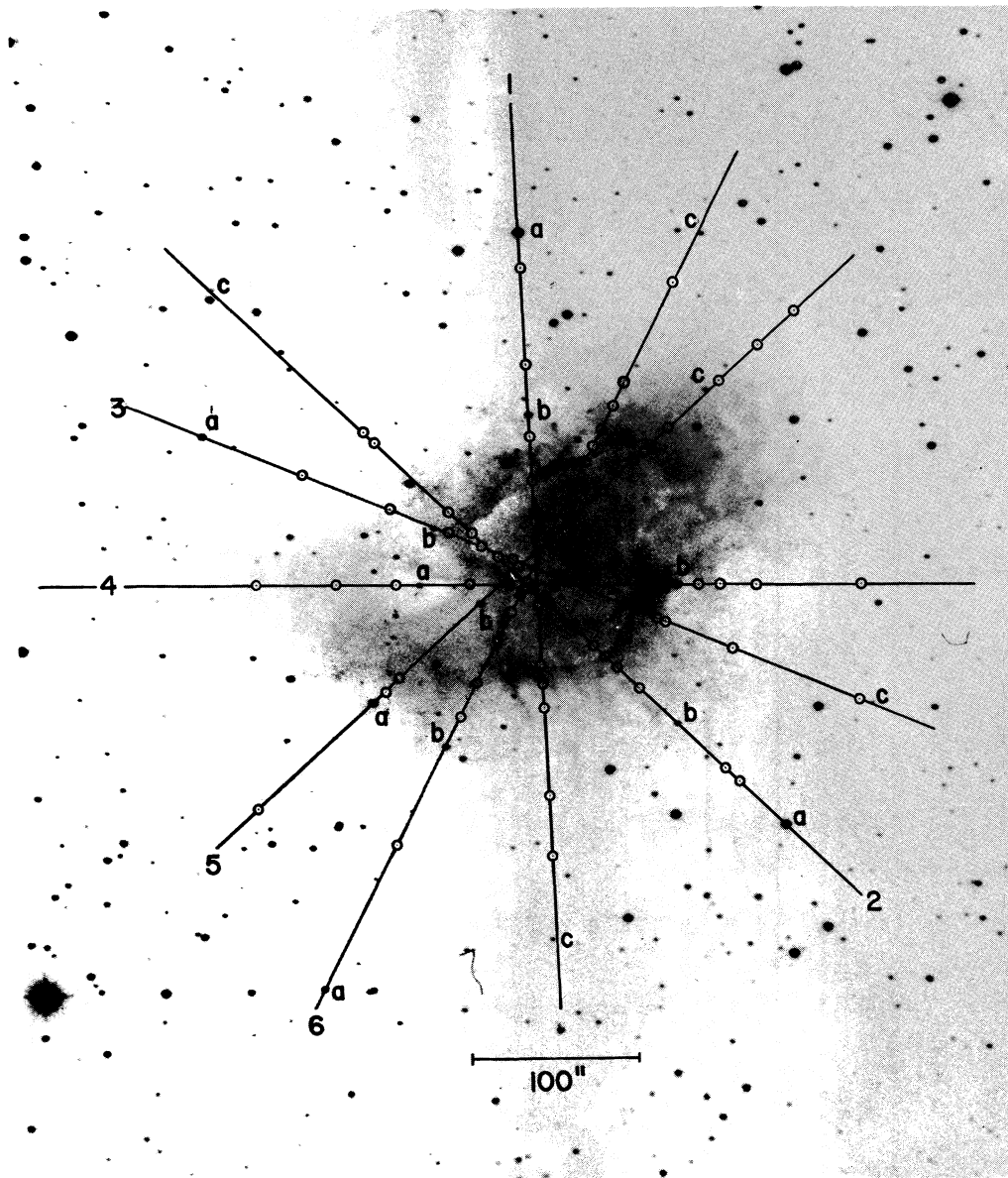


Fig. 3 -- An enlargement of CD 781, numbering the six tracks of the microdensitometer tracings, lettering the calibration stars on each track, marking with small circles the positions of amorphous nebular features measured on all plates, and marking with small squares the least-squares centers s_0 in the equations of condition for the motion of the features on the tracks. North is at the top, east is to the left.

TABLE 2
THE MEASURES OF DISTANCE s FROM A STAR ON THE RECORDER CHARTS

Plate	Stars			Nebula											
	b	c		1	2	3	4	5	6	7	8	9	10	11	12
				Track 1											
99 Dec 24	57	223		15	41	66	84	98	117	126	134	146	174	188	---
99 Dec 26	58	224		15	47	69	84	96	118	126	135	145	174	190	---
1914	57	223		19	44	66	81	97	113	130	137	147	175	197	---
NM 510	58	224		25	41	65	82	93	119	134	143	145	174	204	---
CD 793	58	224		13	43	65	80	92	119	137	143	150	180	189	---
792	59	225		23	45	67	80	93	119	137	144	152	181	195	---
795	58	222		17	44	66	78	92	112	138	143	148	177	192	---
785	58	---		0	44	67	80	92	119	137	143	150	181	205	---
794	58	---		19	45	66	81	93	120	138	143	152	175	198	---
786	58	223		18	46	66	78	92	119	137	144	152	180	195	---
787	58	224		6	43	67	79	92	119	137	144	148	177	202	---
791	59	---		28	45	68	81	93	120	138	144	151	180	201	---
782	59	224		12	44	67	80	93	120	138	144	152	177	201	---
781	59	224		8	43	66	81	93	120	138	144	152	179	195	---
				Track 2											
99 Dec 24	47	247		176	175	146	130	122	116	87	82	77	65	23	20
99 Dec 26	47	249		176	172	146	130	122	114	87	82	76	64	25	24
1914	47	247		178	175	146	133	122	114	86	82	76	64	28	25
NM 510	46	248		178	174	145	133	124	110	90	82	74	64	31	28
CD 793	46	247		185	176	146	133	124	109	83	78	74	63	27	23
792	47	249		178	175	145	135	124	109	83	78	73	64	27	22
795	47	249		182	176	145	135	124	111	83	79	73	64	26	14

TABLE 2 (continued)

THE MEASURES OF DISTANCE s FROM A STAR ON THE RECORDER CHARTS

Plate	Stars			Nebula												
	b	c		1	2	3	4	5	6	7	8	9	10	11	12	
785	47	248		186	176	144	134	123	109	82	78	72	65	27	20	
794	47	248		180	177	145	135	124	108	83	79	73	63	27	25	
786	47	247		181	178	145	135	125	110	83	78	73	66	28	24	
787	47	249		177	173	144	135	124	109	83	79	74	64	27	23	
791	47	248		182	176	145	137	124	110	83	78	73	63	27	19	
782	47	249		181	178	145	135	124	110	83	78	74	64	27	25	
781	47	248		181	178	144	134	124	109	83	79	74	64	29	21	
Track 2 (continued)																
Track 3																
99 Dec 24	78	230		39	69	87	92	109	143	156	158	181	222	---	---	
99 Dec 26	79	229		44	64	87	91	109	143	156	160	183	223	---	---	
1914	80	230		33	68	87	99	108	144	156	160	182	213	---	---	
NM 510	80	230		38	66	86	94	107	144	155	157	178	216	---	---	
CD 793	80	230		31	64	86	97	107	144	156	158	182	222	---	---	
792	78	230		42	65	84	96	107	145	156	159	181	225	---	---	
795	79	229		23	63	85	96	108	144	156	158	182	221	---	---	
785	80	230		44	67	87	96	106	145	155	158	180	218	---	---	
794	80	230		35	65	85	96	107	145	156	159	183	236	---	---	
786	78	230		43	67	84	97	106	145	156	159	179	225	---	---	
787	80	230		35	65	87	98	107	145	155	158	180	220	---	---	
791	81	232		35	67	88	97	107	146	158	160	183	223	---	---	
782	80	230		40	65	85	95	106	145	156	159	181	216	---	---	
781	80	230		31	64	85	96	104	145	156	159	181	238	---	---	

TABLE 2 (continued)
 THE MEASURES OF DISTANCE s FROM A STAR ON THE RECORDER CHARTS

Plate	Stars			Nebula												
	b	c		1	2	3	4	5	6	7	8	9	10	11	12	13
Track 4																
99 Dec 24	82	---		-39	-22	-5	18	28	33	53	74	76	88	92	103	125
99 Dec 26	83	---		-39	-24	-4	18	29	33	55	75	77	88	92	104	136
	1914	81	---	-58	-25	-6	17	28	32	53	74	76	88	92	103	134
	NM 510	82	---	-49	-30	-7	16	29	31	53	76	78	88	94	107	150
	CD 793	81	---	-59	-27	-7	16	29	31	52	75	77	89	96	108	132
	792	81	---	-49	-25	-8	16	28	30	53	75	78	89	96	108	140
	795	81	---	-63	-27	-7	16	28	30	53	75	77	89	96	107	145
	785	81	---	-46	-26	-8	16	28	30	53	75	78	89	95	108	130
	794	82	---	-47	-27	-8	16	29	32	54	75	79	90	97	107	142
	786	81	---	-41	-28	-7	16	29	32	53	75	78	89	95	107	149
	787	81	---	-48	-26	-7	16	28	32	53	75	77	88	96	106	144
	791	82	---	-46	-25	-8	16	29	32	53	76	78	89	96	106	134
	782	81	---	-53	-27	-8	16	28	31	53	77	78	89	96	107	138
	781	81	---	-62	-26	-8	16	29	31	52	75	78	89	96	107	148
Track 5																
99 Dec 24	47	145		-42	9	15	61	66	97	110	119	132	148	159	177	---
99 Dec 26	47	146		-50	9	16	61	67	97	111	119	127	148	160	172	---
	1914	47	146	-46	7	17	61	67	94	113	121	131	150	160	177	---
	NM 510	45	146	-47	8	18	60	64	99	112	116	131	150	158	171	---
	CD 793	46	145	-48	6	11	61	63	100	113	118	128	149	160	173	---
	792	46	145	-52	6	12	60	64	100	113	117	127	150	165	178	---
	795	47	146	-48	6	12	60	63	99	112	117	128	149	165	183	---

TABLE 2 (continued)

THE MEASURES OF DISTANCE s FROM A STAR ON THE RECORDER CHARTS

Plate	Stars			Nebula												
	b	c		1	2	3	4	5	6	7	8	9	10	11	12	13
785	46	146		-51	6	12	60	64	99	114	117	128	150	158	166	---
794	47	145		-50	6	13	60	63	99	113	117	127	151	169	187	---
786	47	146		-33	6	12	60	63	99	113	117	127	148	160	172	---
787	47	146		-56	6	10	60	64	99	112	117	126	150	165	196	---
791	47	146		-54	6	11	60	64	99	113	118	126	149	166	189	---
782	47	145		-52	5	12	61	64	100	113	118	129	151	176	191	---
781	47	146		-44	6	12	60	63	100	114	118	128	151	177	186	---
Track 5 (continued)																
99 Dec 24	87	268		59	98	110	120	131	144	178	181	189	195	203	214	238
99 Dec 26	87	269		52	98	110	121	132	144	177	181	189	196	204	214	253
1914	88	270		55	97	109	120	137	146	180	184	192	198	207	218	241
NM 510	87	270		52	98	109	123	134	147	180	187	192	199	214	219	252
CD 793	86	268		47	93	107	123	131	145	178	186	193	199	207	215	248
792	88	270		43	98	109	124	134	145	180	189	194	199	209	217	251
795	87	268		46	97	107	122	133	144	179	188	194	199	208	215	251
785	86	268		73	95	107	122	132	144	179	187	192	199	208	216	257
794	87	268		49	96	108	123	132	145	179	187	193	199	208	216	253
786	86	268		46	95	106	121	133	145	179	187	193	199	208	216	245
787	88	270		57	98	109	124	133	146	181	189	195	201	209	219	258
791	86	267		52	94	106	122	133	144	178	186	192	198	207	217	251
782	87	269		49	97	109	122	133	145	180	188	193	200	208	216	252
781	86	268		53	97	108	122	133	145	179	188	193	198	208	217	249
Track 6																

TABLE 3

MEASURES OF DISTANCE s FROM MEANS OF THE 8^m AND THE 3^m DEVELOPMENTS

Exp.	Stars			Nebula													
	b	c		1	2	3	4	5	6	7	8	9	10	11	12	13	
	Track 1																
40 ^m	58.5	223.0	14.5	44.0	66.5	79.0	92.5	116.0	138.0	143.5	150.0	177.0	196.5	---	---	---	
20 ^m	58.5	224.5	14.5	44.0	67.0	79.5	92.5	119.0	137.0	144.0	150.0	179.0	198.5	---	---	---	
10 ^m	58.0	223.5	15.5	44.5	65.5	79.0	92.0	119.0	137.0	143.5	151.0	180.0	192.0	---	---	---	
	Track 2																
40 ^m	47.0	249.0	181.5	177.0	145.0	135.0	124.0	110.5	83.0	78.5	73.5	64.0	26.5	19.5	---	---	
20 ^m	47.0	249.0	177.5	174.0	144.5	135.0	124.0	109.0	83.0	78.5	73.5	64.0	27.0	22.5	---	---	
10 ^m	46.5	247.0	183.0	177.0	145.5	134.0	124.5	109.5	83.0	78.0	73.5	64.5	27.5	23.5	---	---	
	Track 3																
40 ^m	79.5	229.5	31.4	64.0	85.0	95.5	107.0	144.5	156.0	158.5	181.5	218.5	---	---	---	---	
20 ^m	79.0	230.0	38.5	65.0	85.5	97.0	107.0	145.0	155.5	158.5	180.5	222.5	---	---	---	---	
10 ^m	79.0	230.0	37.0	65.5	85.0	97.0	106.5	144.5	156.0	158.5	180.5	223.5	---	---	---	---	

TABLE 3 (continued)
 MEASURES OF DISTANCE s FROM MEANS OF THE 8^m AND THE 3^m DEVELOPMENTS

Exp.	Stars	1	2	3	4	5	6	7	8	9	10	11	12	13	
b	c	Nebula													
Track 4															
40 ^m	81.0	---	-58.0	-27.0	-7.5	16.0	28.0	30.5	53.0	76.0	77.5	89.0	96.0	107.0	141.5
20 ^m	81.5	---	-47.5	-25.0	-8.0	16.0	28.5	31.0	53.0	75.5	78.0	89.0	96.0	107.0	137.0
10 ^m	81.0	---	-50.0	-27.5	-7.0	16.0	29.0	31.5	52.5	75.0	77.5	89.0	95.5	107.5	140.5
Track 5															
40 ^m	47.0	145.5	-50.0	5.5	12.0	60.5	63.5	99.5	112.5	117.5	128.5	150.0	170.5	187.0	---
20 ^m	46.5	145.5	-54.0	6.0	11.0	60.0	64.0	99.5	112.5	117.0	126.5	150.0	165.0	187.0	---
10 ^m	46.5	145.5	-40.5	6.0	11.5	60.5	63.0	99.5	113.0	117.5	127.5	148.5	160.0	172.5	---
Track 6															
40 ^m	87.0	268.5	47.5	97.0	108.0	122.0	133.0	144.5	179.5	188.0	193.5	199.5	208.0	215.5	251.5
20 ^m	88.0	270.0	50.0	98.0	109.0	124.0	133.5	145.5	180.5	189.0	194.5	200.0	209.0	218.0	254.5
10 ^m	86.0	268.0	46.5	94.0	106.5	122.0	132.0	145.0	178.5	186.5	193.0	199.0	207.5	215.5	246.5

TABLE 4
MEASURES OF DISTANCE \underline{s} FROM MEANS OF THE 10^m AND 40^m EXPOSURES

Dev.	Stars			Nebula												
	b	c		1	2	3	4	5	6	7	8	9	10	11	12	13
				Track 1												
8 ^m	58.0	223.0	15.0	43.5	65.5	79.0	92.0	115.5	137.5	143.0	149.0	178.5	190.5	---	---	---
5 ^m	58.0	---	9.5	44.5	66.5	80.5	92.5	119.5	137.5	143.0	151.0	178.0	201.5	---	---	---
3 ^m	58.5	223.5	15.0	45.0	66.5	79.0	92.5	119.5	137.5	144.0	152.0	178.5	198.0	---	---	---
				Track 2												
8 ^m	46.5	248.0	183.5	176.0	145.5	134.0	124.0	110.0	83.0	78.5	73.5	63.5	26.5	18.5	---	---
5 ^m	47.0	248.0	183.0	176.5	144.5	134.5	123.5	108.5	82.5	78.5	72.5	64.0	27.0	22.5	---	---
3 ^m	47.0	248.0	181.0	178.0	145.0	135.0	124.5	110.0	83.0	78.0	73.5	65.0	27.5	24.5	---	---
				Track 3												
8 ^m	79.5	229.5	27.0	63.5	85.5	96.5	107.5	144.0	156.0	158.0	182.0	221.5	---	---	---	---
5 ^m	80.0	230.0	39.5	66.0	86.0	96.0	106.5	145.0	155.5	159.5	181.5	227.0	---	---	---	---
3 ^m	79.0	230.0	41.5	66.0	84.5	96.0	106.0	145.0	156.0	159.0	180.0	220.5	---	---	---	---

TABLE 4 (continued)
 MEASURES OF DISTANCE s FROM MEANS OF THE 10^m AND 40^m EXPOSURES

Dev.	Stars			Nebula													
	b	c		1	2	3	4	5	6	7	8	9	10	11	12	13	
	Track 4																
8 ^m	81.0	---		-61.0	-27.0	-7.0	16.0	28.5	30.5	52.5	75.0	77.0	89.0	96.0	107.5	138.5	
5 ^m	81.5	---		-46.5	-26.5	-8.0	16.0	28.5	31.0	53.5	75.0	78.5	89.5	96.0	107.5	136.0	
3 ^m	81.0	---		-47.0	-27.5	-7.5	16.0	28.5	31.5	53.0	76.0	78.0	89.0	95.5	107.0	143.5	
	Track 5																
8 ^m	46.5	145.5	-48.0	6.0	11.5	60.5	63.0	99.5	112.5	117.5	128.0	149.0	162.5	178.0	---	---	
5 ^m	46.5	145.5	-50.5	6.0	12.5	60.0	63.5	99.0	113.5	117.0	127.5	150.5	163.5	176.5	---	---	
3 ^m	47.0	145.5	-42.5	5.5	12.0	60.5	63.5	99.5	113.0	117.5	128.0	149.5	168.0	171.5	---	---	
	Track 6																
8 ^m	86.5	268.0	46.5	95.0	107.0	122.5	132.0	144.5	178.5	187.0	193.5	199.0	207.5	215.0	249.5		
5 ^m	86.5	268.0	61.0	95.5	107.5	122.5	132.0	144.5	179.0	187.0	192.5	199.0	208.0	216.0	255.0		
3 ^m	86.5	268.5	47.5	96.0	107.5	121.5	133.0	145.0	179.5	187.5	193.0	199.5	208.0	216.0	248.5		

TABLE 5
 MEAN VALUE OF \underline{s} AND Δs FROM 1904.9 TO 1963.1

Stars		Nebula												
b	c	1	2	3	4	5	6	7	8	9	10	11	12	13
Track 1														
1963.1	58.4	223.7	14.4	44.2	66.5	79.8	92.5	118.7	137.5	143.6	150.7	178.7	197.3	---
1904.9	57.3	223.3	16.3	44.0	67.0	83.0	97.0	116.0	127.3	135.3	146.0	174.3	191.7	---
Δs	+1.1	+0.4	-1.9	+0.2	-0.5	-3.2	-4.5	+2.7	+10.2	+8.3	+4.7	+4.4	+5.6	---
Track 2														
1963.1	46.9	248.2	181.3	176.3	144.8	134.8	124.0	109.4	82.9	78.4	73.3	64.0	27.2	21.6
1904.9	47.0	247.7	176.7	174.0	146.0	131.0	122.0	114.7	86.7	82.0	76.3	64.3	25.3	23.0
Δs	-0.1	+0.5	+4.6	+2.3	-1.2	+3.8	+2.0	-5.3	-3.8	-3.6	-3.0	-0.3	+1.9	-1.4
Track 3														
1963.1	79.6	230.1	35.9	65.2	85.6	96.4	106.5	144.9	156.0	158.7	181.2	224.4	---	---
1904.9	79.0	229.7	38.7	67.0	87.0	94.0	108.7	143.3	156.0	159.3	182.0	219.3	---	---
Δs	+0.6	+0.4	-2.8	-1.8	-1.4	+2.4	-2.2	+1.6	0.0	-0.6	-0.8	+5.1	---	---

TABLE 5 (continued)
 MEAN VALUE OF \bar{s} AND Δs FROM 1904.9 TO 1963.1

	Stars			Nebula												
	b	c		1	2	3	4	5	6	7	8	9	10	11	12	13
1963.1	81.2	---		-51.4	-26.4	-7.6	16.0	28.5	31.1	52.9	75.3	77.8	89.0	95.9	107.1	140.2
1904.9	82.0	---		-45.3	-23.7	-5.0	17.7	28.3	32.7	53.7	74.3	76.3	88.0	92.0	103.3	131.7
$\Delta \bar{s}$	-0.8	---		-6.1	-2.7	-2.6	-1.7	+0.2	-1.6	-0.8	+1.0	+1.5	+1.0	+3.9	+3.8	+8.5
Track 4																
1963.1	46.7	145.6		-48.8	5.9	11.7	60.2	63.5	99.4	113.0	117.4	127.4	149.8	166.1	182.1	---
1904.9	47.0	145.7		-46.0	8.3	16.0	61.0	66.7	96.0	111.3	119.7	130.0	148.7	159.7	175.3	---
$\Delta \bar{s}$	-0.3	-0.1		-2.8	-2.4	-4.3	-0.8	-3.2	+3.4	+1.7	-2.3	-2.6	+1.1	+6.4	+6.8	---
Track 5																
1963.1	86.7	268.4		51.5	96.0	107.6	122.5	132.7	144.8	179.2	187.5	193.2	199.1	208.0	216.4	251.5
1904.9	87.3	269.0		55.3	97.7	109.7	120.3	133.3	144.7	178.3	182.0	190.0	196.3	204.7	215.3	244.0
$\Delta \bar{s}$	-0.6	-0.6		-3.8	-1.7	-2.1	+2.2	-0.6	+0.1	+0.9	+5.5	+3.2	+2.8	+3.3	+1.1	+7.5
Track 6																

TABLE 6

LEAST SQUARES SOLUTIONS OF THE NORMAL EQUATIONS FOR THE CENTERS AND TIMES OF EXPANSION

Track	PA (1963) (degrees)	Group	$s_0 + m.e.$ (mm)	$58.2 t + m.e.$ (years before 1963)	PA - 125° (degrees)	Group	$58.2 \bar{t}$ (years before 1963)
1	2	all	$91.4 + 14.6$	$489 + 166$			
		central	$100.3 + 8.7$	$285 + 88$			
2	47	all	$103.9 + 14.9$	$423 + 278$	-86	all	617
		central	$108.3 + 11.4$	$279 + 205$	(near minor axis)	central	237
3	68	all	$126.3 + 14.1$	$939 + 356$			
		central	$124.8 + 14.6$	$146 + 528$			
4	90	all	$43.5 + 5.7$	$837 + 91$			
		central	$49.4 + 5.5$	$930 + 159$			
5	132	all	$86.2 + 14.7$	$786 + 236$	0	all	842
		central	$100.4 + 15.4$	$504 + 336$	(near major axis)	central	712
6	152	all	$138.8 + 9.2$	$904 + 161$			
		central	$143.3 + 10.9$	$702 + 228$			

constants along each track starting at a time $(1963.1 - 1904.9) \underline{t}$ years before 1963.1 from a center \underline{s}_0 , the equations of condition for determining \underline{s}_0 and \underline{t} have the form $\Delta \underline{s} \cdot \underline{t} + \underline{s}_0 = \underline{s}$. The normal equations are solved for \underline{s}_0 and \underline{t} by least squares, and the results are given in Table 6. Each track has been treated twice, first for all of the measures and, second, for the inner $\underline{n} - 4$ measures, omitting the two outermost measures on either side of the nebula. Table 6 shows that $58.2 \underline{t}$ (central group) : $58.2 \underline{t}$ (all measures) : $(1963 - 1054) = 474 : 730 : 909$. This result suggests that the expansion of the amorphous mass of the Crab Nebula is accelerating, and that the inner parts are accelerating more than the outer parts. Alternatively brief initial accelerations are followed by constant velocities for lifetimes $58.2 \underline{t}$ years. In the latter case the accelerations occurred $909 - 58.2 \underline{t}$ years after the supernova of 1054 A.D. Another way of looking at either of these alternatives is to say that the Crab Nebula is changing its physiognomy. If each feature has contributed the same proportion of the total flux for the last 60 years, the bell-shape profile of the intensity versus the diameter is currently growing blunter at the top.

Table 6 suggests that the current accelerations are smallest near the major axis of the nebula or, alternatively, that the lifetimes of constant velocity are greatest there. The major axis of the filamentary shell is near $\underline{PA} = 122^\circ$ (Münch 1958), but the position angle of the amorphous mass varies grossly according to isophotic level in Woltjer's (1957) map. It reflects the S-shape that Baade (1942) noted inside the filamentary shell, and becomes about 135° in the periphery outside the filamentary shell.

Duncan's (1939) center of filamentary expansion (cf. Figure 1) is inside a small hexagon the vertices of which are defined by the track centers \underline{s}_0 in Table 6, so the present data do not give a significantly different center of expansion. The hexagon also includes Baade's (1942) center of the elliptical boundary of the filamentary shell.

If the amorphous structure is expanding from a single center off the tracks (such as Duncan's center), the components of the expansion of the tracks are smaller fractions of the radial expansion as the center is approached. This means that the inner parts are moving faster on the plane of the sky than the track components show. Even the full components on the plane of the sky near the center are likely to be partial components of the spatial motions, because the present measures presumably integrate on lines of sight through the volume. (Duncan's measures of proper motions were made near the perimeter of the ellipse that bounds the filamentary system, and presumably they give practically the full components of the spatial motions.)

In conclusion, a fairly extensive set of amorphous features in the Crab Nebula has been measured in order to detect positional shift, relative to field stars, over a period of about 60 years. The shifts are predominantly in the sense of expansion from a stationary center of the nebula. Current accelerations or short lifetimes ($60 \text{ years} < 58.2 \underline{t} < 900 \text{ years}$) are evident, especially near the center. The expansion of the outer amorphous structure in the vicinity of the embedded filamentary shell probably agrees with the shell's expansion.

Throughout this paper the use of the terms motion and acceleration apply to material particles in speaking of the filamentary system. But in the amorphous system, to which all of the new data refer, the terms are applied to luminous fronts and features that may reflect the evolution of the magnetic field.

REFERENCES

- Baade, W. 1942, Ap. J., 96, 188.
 ----- . 1956, B.A.N., 12, 312.
- Deutsch, A. N., and Lavdovsky, V. V. 1940, Pulkova Obs. Circ., No. 30, 21.
- Duncan, J. C. 1921, Proc. N.A.S., 7, 179.
 ----- . 1939, Ap. J., 89, 482.
- Gurzadyan, G. A. 1960, Dokl. Akad. Nauk U.S.S.R., 130, 47; Soviet Phys. -- Dokl.,
5, 7.
- Hiltner, W. A. 1957, Ap. J., 125, 300.
- Lampland, C. O. 1921, Pub. A.S.P., 33, 79.
- Little, A. G. 1963, Ap. J., 137, 164.
- Martel, M. T. 1958, Sup. Ann. d'Ap., No. 7, 32.
- Mayall, N. U. 1937, Pub. A.S.P., 49, 101.
 ----- . 1962, Science, 137, 91.
- Münch, G. 1958, Revs. Mod. Phys., 30, 1042.
- Oort, J. H., and Walraven, T. 1956, B.A.N., 12, 285.
- Sanford, R. F. 1919, Pub. A.S.P., 31, 108.
- Shajn, G. A., Pikelner, S. B., and Ikhsanov, R. N. 1955, A.J.U.S.S.R. 32, 395.
- Shklovsky, I. S. 1953, Dokl. Akad. Nauk U.S.S.R., 90, 983.
- Slipher, V. M. 1916, Pub. A.S.P., 28, 191.
- Woltjer, L. 1957, B.A.N., 13, 301.
 ----- . 1958, B.A.N., 14, 39.